Polymer Chemistry

ROYAL SOCIETY OF CHEMISTRY

PAPER

View Article Online
View Journal | View Issue

Check for updates

Cite this: *Polym. Chem.*, 2022, **13**, 6054

Exploring the potential of polypeptide–polypeptoide hybrid nanogels for mucosal delivery†

Tao Xu,[a,b] Dimitrios Skoulas, *[c] Dawei Ding,[b] Sally-Ann Cryan [a,d,e] and Andreas Heise *[c,d,e]

Amphiphilic nanoparticles with high drug loading capacity and mucus penetration properties are attractive for the delivery of potent hydrophobic drugs across the mucosal barrier in tumor therapy. In this study we report a facile strategy towards biocompatible and tumour microenvironment responsive nanogels, capable of controlling the mucosal delivery and release of a model dye. Polypeptide–polypeptoide hybrid nanogels were obtained by the chain extension of corona-forming poly(sarcosine) with *N*-carboxyanhydrides (NCA) of phenylalanine and cystine as a core crosslinker. The nanogels exhibited a suitable size range of around 100 nm and a spherical morphology as monitored by dynamic light scattering (DLS), transmission electron microscopy (TEM) and nanoparticle tracking analysis (NTA). They further showed a reduction-responsive behaviour through the cleavage of the cystine disulfide core crosslinks by glutathione at concentrations present in the intracellular environment as well as a lack of cytotoxicity against both cancerous and non-cancerous cell lines. Lead nanogels facilitated an enhanced transport of a model hydrophobic dye across artificial mucus compared to the dye alone with a reduction sensitive release in the presence of glutathione. This work provides a facile strategy for the synthesis of responsive nanomedicines in anti-cancer therapy where mucosal barriers have to be overcome.

Received 30th August 2022,
Accepted 9th October 2022

DOI: 10.1039/d2py01126c

rsc.li/polymers

Open Access Article. Published on 10 October 2022. Downloaded on 7/19/2025 11:20:55 AM.
This article is licensed under a Creative Commons Attribution-NonCommercial 3.0 Unported Licence.

Introduction

The last decade has witnessed continuously increasing interest in the field of nanomedicine.[1] The use of nanocarriers for the delivery of therapeutic drugs has received specific attention as it offers to overcome well-known biological barriers in drug delivery.[2] These include the delivery of next generation highly potent hydrophobic drugs to difficult-to-deliver-to disease environments as is often encountered in cancer treatment.[3,4] Nanoparticles can be precisely designed to facilitate drug delivery in these settings by carefully engineering their core and surface properties. Nanoparticles with a hydrophobic core for drug loading, ideally allowing a triggered drug release at the disease site, and a hydrophilic surface to permit stability and transport in physiological fluids are desirable. In particular cases, for example drug delivery to tumours in the gastrointestinal tract, mucus penetration properties can improve the drug availability at the tumour site.[5–7] A broad spectrum of different nanosystems has been proposed and tested for therapeutic delivery to date including solid-lipid nanoparticles, liposomes, vesicles, and polymer nanoparticles, among others.[4,8–11] Nanogels have also emerged as a promising class of particles for the delivery of pharmaceuticals. Nanogels are nanosized polymeric materials obtained from selectively core cross-linked networks at an optimised ratio of monomer to crosslinker.[12–15] Their small size combined with the ability to impart a diverse range of properties to nanogels renders them suitable for a wide variety of bio-applications like bio-imaging, tissue engineering and drug and gene delivery.[16–18] In particular, nanogels that respond to the alteration of a stimulus such as pH, temperature or redox are promising candidates as vehicles for drug delivery applications.[19–21] The majority of reported nanogels are based on acrylates obtained by free radical polymerization (FRP),[22,23] reversible addition–fragmentation chain-transfer polymerization (RAFT),[24] atom transfer radical polymerization

[a]*School of Pharmacy and Biomolecular Sciences and Tissue Engineering Research Group, RCSI University of Medicine and Health Sciences, Dublin 2, Ireland*
[b]*College of Pharmaceutical Sciences, Soochow University, 199 Ren'ai Road, Suzhou 215123, China*
[c]*Department of Chemistry, RCSI University of Medicine and Health Sciences, Dublin 2, Ireland. E-mail: andreasheise@rcsi.ie*
[d]*Science Foundation Ireland (SFI) Centre for Research in Medical Devices (CURAM), RCSI, Dublin 2, Ireland*
[e]*AMBER, The SFI Advanced Materials and Bioengineering Research Centre, RCSI, Dublin 2, Ireland*

†Electronic supplementary information (ESI) available: Experimental procedures, additional characterisation of nanogels. See DOI: https://doi.org/10.1039/d2py01126c

This journal is © The Royal Society of Chemistry 2022

Open Access Article. Published on 10 October 2022. Downloaded on 7/19/2025 11:20:55 AM.
This article is licensed under a Creative Commons Attribution-NonCommercial 3.0 Unported Licence.

(ATRP)[25] and emulsion techniques.[26] However, the fully synthetic nature of these materials renders them non-degradable and can cause biocompatibility issues. We are interested in employing nanoparticles from polypeptides as biocompatible and resorbable materials in drug and gene delivery applications.[27–30] Polypeptides are typically obtained by the controlled ring opening polymerization of amino acid *N*-carboxyanhydrides (NCA),[31,32] a technique that has also been applied for the synthesis of responsive nanogels.[33,34] Specifically, the integration of disulfide bonds in the core of nanogels was reported to offer high consistency and reduction-sensitive nanostructures with improved intracellular drug release properties.[35–38] In the reported examples, the direct polymerization of cystine NCA (di-cysteine, dCys-NCA), a readily accessible difunctional NCA, was utilized for the chemical crosslinking of the nanogels.[39,40] The drug release strategy relies on the 500–1000 times higher concentration of the reductive tripeptide glutathione (GSH) in the tumour cytoplasm as compared to the extracellular tumour microenvironment.[41–44] It was demonstrated that the disulfide bonds in these polypeptide nanogels are cleaved in the presence of GSH causing cargo release. This led researchers to study polypeptide nanogels based on a cystine core as vectors for controlled and targeted drug delivery against cancer tissues.[35,37] Introduction of dCys-NCA in polypeptide nanogels was achieved with amine functional poly(ethylene glycol) (PEG-NH_2) rendering the nanogel surface hydrophilic. PEGylation is also a well-established concept to facilitate nanoparticle mucus penetration by reducing the interaction of nanoparticles with the charged components of the mucosal layer.[45,46] However, an increased number of reports have been published pointing out hypersensitivity to PEG as well as its detrimental effects on cell uptake.[47,48] A promising alternative for surface modification of nanoparticles is poly(sarcosine) (PSar), a polypeptoide derived from the *N*-methylated derivative of glycine (sarcosine). Highly hydrophilic PSar has many features that can promote mucosal delivery including neutral surface charge.[49–51] PSar can be conveniently obtained by the polymerisation of its corresponding NCA.[52] In a recent publication, we demonstrated mucus- and tissue-permeating properties of amphiphilic 8 arm star poly(L-glutamic acid-*b*-sarcosine) vectors for mucosal drug delivery.[53]

Here we report the first example of a polypeptide–polypeptoide hybrid nanogel using PSar as a hydrophilic corona. We demonstrate a facile strategy towards biocompatible and tumour microenvironment responsive nanogels, capable of controlling the mucosal delivery and release of a model dye. A series of PSar-*b*-P(Phe-*co*-dCys) nanogels were synthesized by ROP of amino acid NCA. Polypeptide–polypeptoide nanogels were monitored for their structure, size, stimuli-responsiveness, and drug loading ability. Moreover, a lead candidate was selected for further drug delivery and mucus penetration studies. Considering recent efforts in the synthesis of functional polypeptoides,[54–56] the strategy presented here could open an avenue for the design of biocompatible surface functional nanogels difficult to achieve by other techniques.

Results and Discussion

Synthesis and characterisation of polypeptide/polypeptoide hybrid nanogels

NCA monomers of Sar and Phe were obtained by their reaction with triphosgene, while thionyl chloride, a milder chlorinating agent, was utilized for the formation of two L-cystine NCA rings at 0 °C (Schemes S1–S3†). ^{1}H-NMR spectra confirmed the successful synthesis and purity of the NCA monomers (Fig. S2, S4 and S6†). This was further corroborated by the presence of two characteristic ν(C=O) FTIR vibrational NCA bands around 1780 and 1850 cm^{-1} (Fig. S1, S3 and S5†). The synthesis of the hybrid nanogels is depicted in Scheme 1. Allylamine was selected as the initiator for the formation of the PSar block for which a degree of polymerization (DP) of 77 was targeted for all nanogels. When quantitative Sar NCA consumption was reached, verified by FTIR spectroscopy (Fig. S7†), the PSar chain was extended by the addition of a mixture of Phe NCA and dCys NCA. Size exclusion chromatography (SEC) analysis of PSar before chain extension showed a monomodal trace with a dispersity ($Đ$) of <1.1 (Fig. S8†). The total DP of the poly(Phe-*co*-dCys) block was set to 18–19 and 72–74, respectively,

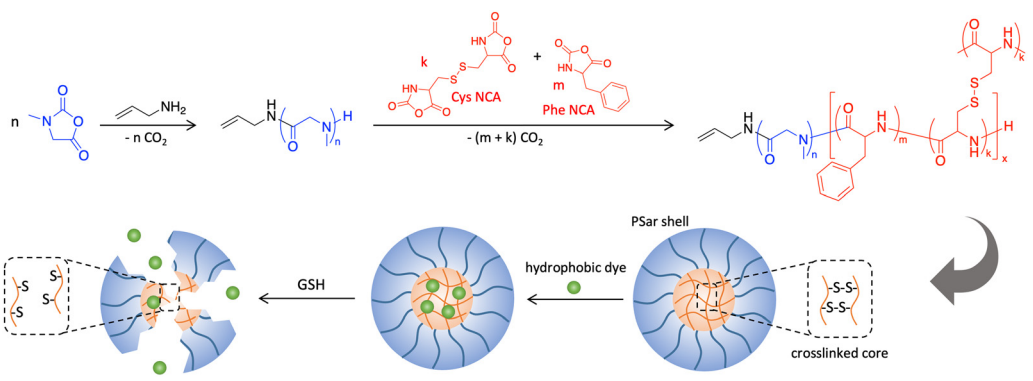

Scheme 1 Synthesis of polypeptide/polypeptoide hybrid nanogels.

Open Access Article. Published on 10 October 2022. Downloaded on 7/19/2025 11:20:55 AM.
This article is licensed under a Creative Commons Attribution-NonCommercial 3.0 Unported Licence.

Table 1 Synthesized PSar-*b*-P(Phe-*co*-dCys) polymers

Entry	DP Sar^{theor}	DP Phe^{theor}	DP dCys^{theor}	Phe/dCys ratio
NG1	77	16	3	5 : 1
NG2	77	12	6	2 : 1
NG3	77	48	24	2 : 1
NG4	77	64	12	5 : 1

while the dCys to Phe molar ratio was varied at 5 : 1 and 2 : 1 for both DP ranges (Table 1). The progress of the chain extension was monitored by the disappearance of the NCA carbonyl signals by FTIR analysis. Notably, the absence of a characteristic FTIR sulfhydryl (–SH) band at 2566 cm^{-1} provides evidence that the disulfide bridges of dCys remained intact during the polymerisation (Fig. S7†). This resulted in the simultaneous crosslinking and formation of the hydrophobic nanogel core during the chain extension.

Quantification of the dCys to Phe ratio in the crosslinked particles was attempted by ^{1}H-NMR spectroscopy. While in DMSO-*d*6 this proved to be impossible due to the overlap of PSar with the copolypeptide block signals, using $CDCl_3$ as a block-selective NMR solvent provided better results. Due to the poor solubility of PSar in $CDCl_3$, its signals are shielded and characteristic monomer signals of Phe (**a** in Fig. 1a) and dCys (**d** in Fig. 1a) are distinguishable in the spectra (Fig. S9–S11†).

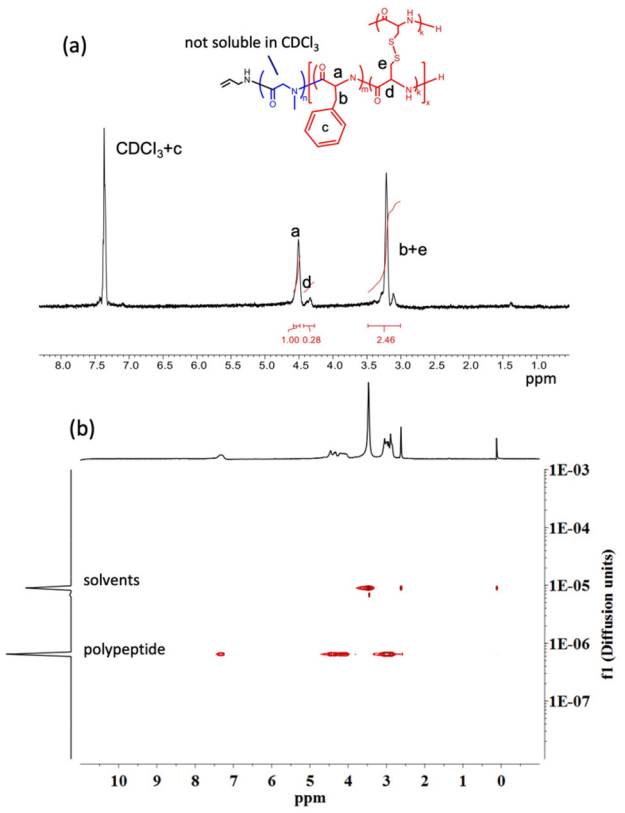

Fig. 1 ^{1}H-NMR (a) and DOSY (b) spectra of NG4 in $CDCl_3$ and DMSO-*d*6.

While the overall quality of the NMR spectra measured under these conditions did not allow an exact calculation of the dCys/Phe ratio, they largely agreed with the monomer feed ratio in Table 1. Most importantly, diffusion-ordered spectroscopy (DOSY) showed a single diffusion coefficient for all polymer signals, suggesting that they belong to the same compound thereby confirming the absence of multiple polymer species (Fig. 1b and Fig. S12†).

All amphiphilic nanogels were lyophilized after synthesis and stored as a dry powder. Fresh dispersions were obtained by dissolving the nanogel powder in 10 mM PBS (pH 7.4) at a concentration of 1 mg ml^{-1}. As evident from TEM analysis, the amphiphilic hybrid nanogels form spherical nanoaggregates in PBS. It is hypothesised that in these nanogel assemblies the hydrophobic cores are shielded from the aqueous environment by PSar coronas as depicted in Scheme 1. Analysis of the nanoparticles using dynamic light scattering (DLS) revealed average hydrodynamic diameters of around 100 nm except for NG1 with a particle size of 143 ± 1.4 nm (Table 2 and Fig. S13†). Size stability upon 100× dilution was confirmed to be exemplary for NG4 (Fig. S14†). Nanoparticle sizes and spherical shapes were confirmed by nanoparticle tracking analysis (NTA) (Table 2 and Fig. S15†). However, TEM images (Fig. 2) and DLS plots suggested some multimodal distributions and relatively high polydispersity indices. With this caveat, no specific dependencies of nanoparticle size on the nanogel block lengths and monomer ratios could be identified. It can be concluded, though, that nanoparticles obtained from nanogels NG2–4 meet the size requirement of around 100 nm for mucus penetration properties.[57]

The reduction-responsive behaviour of the nanogels was evaluated by monitoring their DLS size change in PBS in the presence of 10 mM GSH, thereby mimicking the intracellular reduction environment.[44] As shown in Fig. 3, nanogels in PBS without GSH maintained a constant size over 24 h, which suggests that all four types of nanogels possess good stability. When the nanogels were incubated with GSH, they demonstrated reduction sensitivity evidenced by a significant size increase due to the reductive cleavage of the core disulfide crosslinker. Particles from NG2–4 displayed a DLS size increase between 1.6–5 fold within 24 h, while a 24-fold increase was seen for NG1 (Fig. 3). This might be due to the fact that NG1 has the lowest dCys content (crosslink density) combined with the lowest polypeptide to PSar ratio facilitating better

Table 2 Summary of hybrid nanogel particle size characterisation in 10 mM PBS (pH 7.4) at a concentration of 1 mg ml^{-1}

Entry	*Z*-average (nm)	DLS PDI	NTA (nm)
NG1	143 ± 1.4	0.151 ± 0.023	130 ± 4.7
NG2	91 ± 2.3	0.417 ± 0.055	86 ± 1.2
NG3	108 ± 0.2	0.193 ± 0.002	91 ± 5.0
NG4	106 ± 0.3	0.263 ± 0.008	114 ± 1.9

DLS: dynamic light scattering; NTA: nanoparticle tracking, PDI: polydispersity index. Data reported as mean ± SD (n = 3).

This journal is © The Royal Society of Chemistry 2022

Open Access Article. Published on 10 October 2022. Downloaded on 7/19/2025 11:20:55 AM.
This article is licensed under a Creative Commons Attribution-NonCommercial 3.0 Unported Licence.

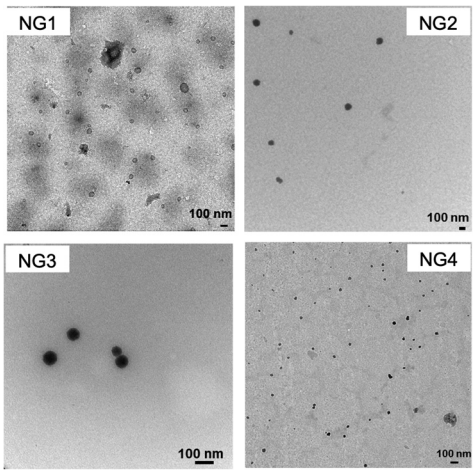

Fig. 2 TEM images (scale bars represent 100 nm) of NG1–4 after the dispersion of dry powder in PBS buffer.

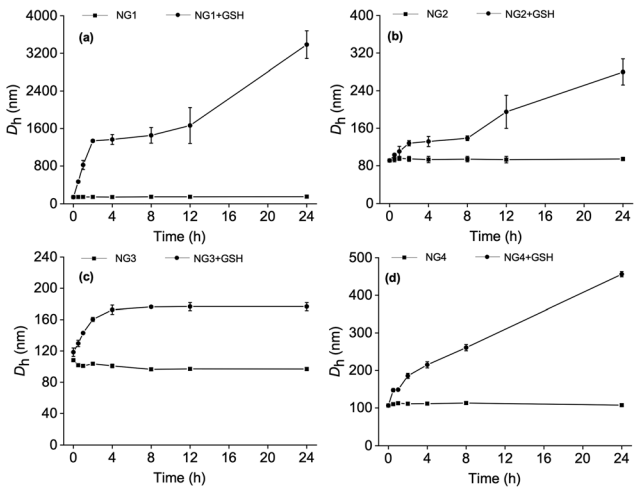

Fig. 3 The change of D_h with time of (a) NG1, (b) NG2, (c) NG3, and (d) NG4 in PBS at pH 7.4 after treatment with 10 mM glutathione (GSH) monitored by DLS (n = 3 ± SD).

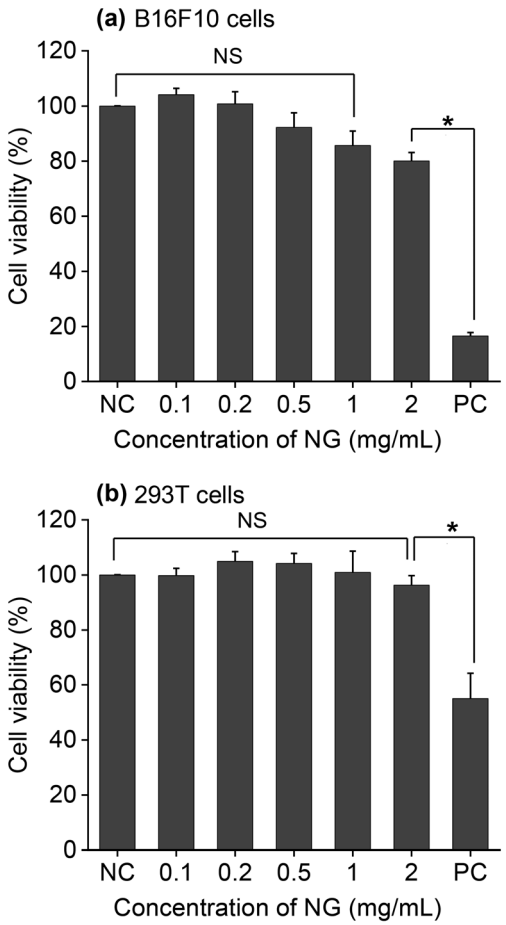

Fig. 4 MTT assays of hybrid nanogel particles from NG4. (a) B16F10 and (b) 293T cells were incubated with nanogels, the negative control (NC: medium) and the positive control (PC: 5% DMSO) for 24 h. Data are presented as average ± standard deviation (n = 3). * P < 0.05. NS indicates no significance.

access of the GSH to the nanogel core. TEM image provided further evidence for the cleavage of NG4, the coexistence of small spherical particles and large irregular aggregates confirmed the disintegration of NG4 *via* the cleavage of the disulfide bridge (Fig. S16†).

Drug delivery potential of hybrid nanogel particles

The results of the previous section confirmed that nanogels from polypeptide/polypeptoide could be obtained in a size range suitable for drug delivery application. Moreover, we demonstrated that they respond to the reductive cleavage of disulfide bonds using a tumour-specific trigger. To validate their potential for therapeutic delivery, NG4 was selected as a prototype considering both GSH responsiveness and its smaller size. First, MTT assays were performed to evaluate the toxicity of the nanogel hybrid particles on the murine melanoma cell line (B16F10) and human embryonic kidney cell line (293T). Fig. 4 shows the results of the cytotoxicity assays as a function of increasing NG4 concentrations (0.1–2 mg ml^{-1}) used to treat the cells. When B16F10 cells were treated, the results confirmed no statistically significant cytotoxicity over the tested concentration range of the unloaded NG4 nanogels compared to the negative control (5% DMSO). B16F10 cells treated with NG4 nanogels also demonstrate a significant viability >85% over a range of treatment concentrations (0.1 to 1 mg mL^{-1}), and viability >80% at 2 mg mL^{-1}.

To model drug loading and release, a hydrophobic dye (IR780) was loaded into the NG4 nanogel using a nanoprecipitation method. The dye loading was first optimised by changing the NG4 to IR780 ratio. It was found that the dye loading (DL) and the encapsulation efficiency (EE) were the highest at 4.5% and 74%, respectively, at an NG4 to IR780 ratio (w/w) of 10 : 1 (Table S1†). In addition, the dye-loaded nanogel size remained around 100 nm by DLS (Fig. S17†). TEM and NTA

Open Access Article. Published on 10 October 2022. Downloaded on 7/19/2025 11:20:55 AM.
This article is licensed under a Creative Commons Attribution-NonCommercial 3.0 Unported Licence.

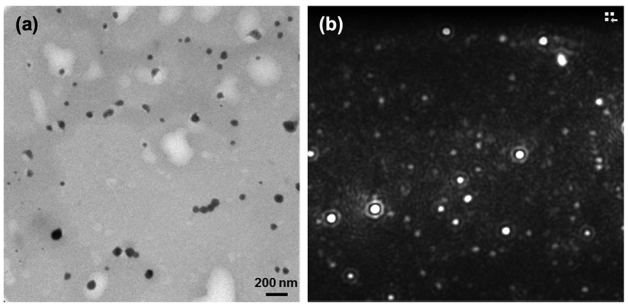

Fig. 5 (a) TEM micrograph (scale bar 200 nm) and (b) still image of nanoparticle tracking analysis (NTA) of NG4 loaded with IR780.

images showed relatively homogeneous nanoparticles with no obvious difference compared to those before dye loading (Fig. 5).

The release profile of IR780 from the cross-linked NG4 nanogel was studied using a dialysis membrane (MWCO: 3500) in PBS (10 mM, pH 7.4) with 10 mM GSH and without any GSH. As observed in Fig. 6, in the absence of GSH the release of IR780 was limited to less than 15% after 72 h. In contrast, in the presence of 10 mM GSH, a concentration mimicking the intracellular environment of the tumour tissue, about 45% of IR780 was steadily released over the same time. This is hypothesised to be due to the breaking of the disulfide bonds inside the core of the nanoaggregates and the swelling of the nanogels. The results suggest that the internally cross-linked hybrid nanogel can minimize the drug loss under extracellular conditions and allow for fast drug release within the target cells in response to intracellular GSH. Hence, the nanogel can act as an "on-demand" drug delivery system for tumour treatment.

Finally, the ability of the IR780 loaded NG4 to penetrate mucus was assessed. Mucus is a viscoelastic and adhesive hydrogel that represents a substantial barrier to mucosal drug delivery.[57] In order to penetrate mucus, synthetic nanoparticles must avoid adhesion to mucin fibres and be small enough to avoid significant steric hindrance by the dense fibre mesh. Mucus penetration was measured in a Transwell-Snapwell diffusion chamber across a polycarbonate membrane (pore size 3 μm) covered with a layer of artificial mucus.[53] NG4-IR780 and control samples (IR780 alone) were added to the apical side of the chamber and samples were withdrawn from the basolateral compartment every 60 min for 240 min. The quantity of IR780 present in the basolateral compartment was measured by UV-Vis spectroscopy and quantified against a calibration curve. Notably, NG4-IR780 could facilitate the delivery of an average of 4.4 μg IR780 across the mucous layer within 4 h (Fig. 7). Significantly the dye alone could hardly pass through the mucus due to its hydrophobicity (0.25 μg transported over 4 hours). The results highlight that the nanogel can effectively minimize the adhesive interactions between mucin and the nanoparticles by reducing the hydrophobic or electrostatic interactions *via* its hydrophilic and charge-neutral PSar shell. This renders the hybrid nanogels promising drug delivery systems for the treatment of a variety of diseases of the epithelium including rectal and intestinal cancers.

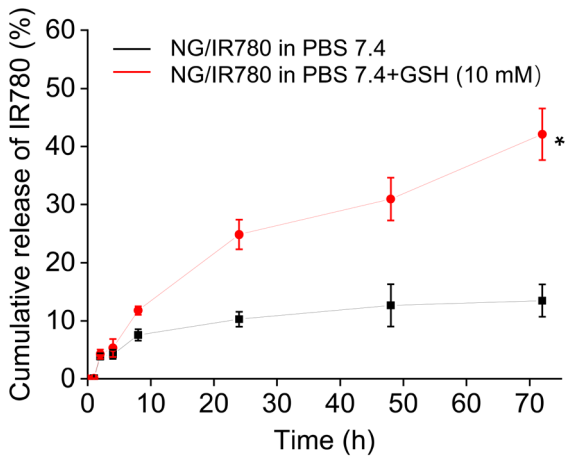

Fig. 6 *In vitro* IR780 release from IR780 loaded NG4 nanogels in PBS with and without 10.0 mM GSH at pH 7.4, 37 °C. Data are presented as average ± standard deviation (n = 3). * $P < 0.05$.

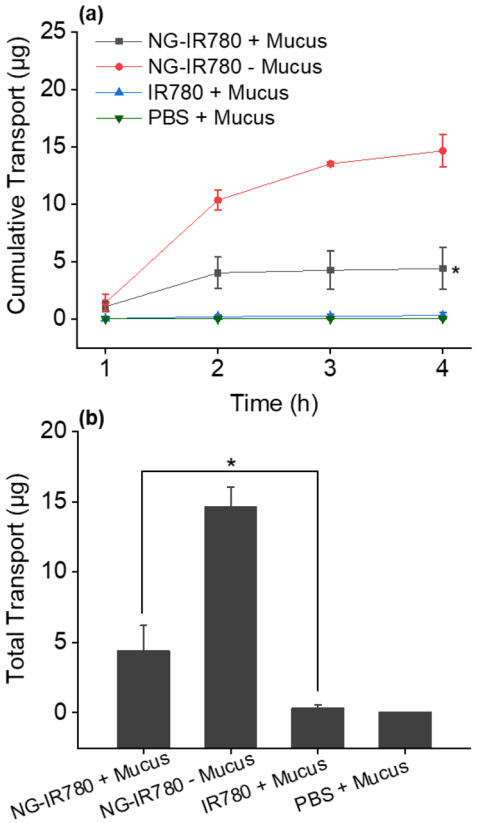

Fig. 7 (a) Transport of NG/IR780 across a polycarbonate membrane was measured in the presence and absence of artificial mucus. PBS with mucus and IR780 with mucus were used as the control. (b) Total transport of NG/IR780 after 4 h. Data are presented as average ± standard deviation (n = 3). * indicates $P < 0.05$.

This journal is © The Royal Society of Chemistry 2022

Open Access Article. Published on 10 October 2022. Downloaded on 7/19/2025 11:20:55 AM. This article is licensed under a Creative Commons Attribution-NonCommercial 3.0 Unported Licence.

Conclusions

In this study, a novel family of reduction sensitive core-cross-linked nanogels based on a PSar-*b*-P(Phe-*co*-dCys) polypeptide/polypeptoide hybrid composition was prepared. The nanogel exhibited a suitable size range of around 100 nm and non-cytotoxicity against both cancerous and non-cancerous cell lines. Importantly, the nanogels facilitated the transport of a model hydrophobic dye across artificial mucus with a reduction sensitive release in the presence of GSH, a trigger enriched in tumor cells. Consequently, this work provides a facile strategy for the synthesis of GSH-responsive nanomedicines for anticancer therapy and mucosal delivery. Encouraged by the present findings, further research will be conducted to examine these nanocarriers both *in vitro* and *in vivo* for the improvement of oncologic photodynamic therapy. The co-delivery of immune agents and drugs as multiple therapeutic payloads to cancerous tissues for synergistic antitumor treatment will be explored.

Author Contributions

T. X.: investigation, writing – original draft. D. S.: conceptualisation, supervision, writing – original draft. D. D.: funding acquisition, supervision, writing – review and editing. S.-A. C.: supervision, resources, funding acquisition, writing – review and editing. A. H.: supervision, methodology, resources, writing – review and editing.

Conflicts of interest

There are no conflicts to declare.

Acknowledgements

This project has received funding from the European Union's Horizon 2020 research and innovation programme under grant agreement No. 883951. Support from the Priority Academic Program Development of the Jiangsu Higher Education Institutes (PAPD), China is acknowledged. Open access funding has been provided by IReL.

References

1 S. Soares, J. Sousa, A. Pais and C. Vitorino, *Front. Chem.*, 2018, **6**, 360.
2 H. Ragelle, F. Danhier, V. Préat, R. Langer and D. G. Anderson, *Expert Opin. Drug Delivery*, 2017, **14**, 851.
3 S. Tran, P. J. DeGiovanni, B. Piel and P. Rai, *Clin. Transl. Med.*, 2017, **6**, 44.
4 A. Z. Mirza and F. A. Siddiqui, *Int. Nano Lett.*, 2014, **4**, 94.
5 F. Lv, J. Wang, H. Chen, L. Sui, L. Feng, Z. Liu, Y. Liu, G. Wei and W. Lu, *J. Controlled Release*, 2021, **336**, 572.
6 V. V. Khutoryanskiy, *Macromol. Biosci.*, 2011, **11**, 748.
7 G. P. Andrews, T. P. Laverty and D. S. Jones, *Eur. J. Pharm. Biopharm.*, 2009, **71**, 505.
8 H. M. Abdel-Mageed, A. E. Abd El Aziz, S. A. Mohamed and N. Z. AbuelEzz, *J. Microencapsulation*, 2022, **39**, 72.
9 S. Su and P. M. Kang, *Nanomaterials*, 2020, **10**, 656.
10 E. Beltrán-Gracia, A. López-Camacho, I. Higuera-Ciapara, J. B. Velázquez-Fernández and A. A. Vallejo-Cardona, *Cancer Nanotechnol.*, 2019, **10**, 11.
11 W. B. Liechty and N. A. Peppas, *Eur. J. Pharm. Biopharm.*, 2012, **80**, 241.
12 T. Kaewruethai, C. Laomeephol, Y. Pan and J. A. Luckanagul, *Gels*, 2021, **7**, 228.
13 B. Stawicki, T. Schacher and H. Cho, *Gels*, 2021, **7**, 63.
14 N. K. Preman, S. Jain and R. P. Johnson, *ACS Omega*, 2021, **6**, 5075.
15 Z. Zhang, G. Hao, C. Liu, J. Fu, D. Hu, J. Rong and X. Yang, *Food Res. Int.*, 2021, **147**, 110564.
16 X. Qin, C. Wu, D. Niu, L. Qin, X. Wang, Q. Wang and Y. Li, *Nat. Commun.*, 2021, **12**, 5243.
17 W. Zhang, B. Du, M. Gao and C. H. Tung, *ACS Nano*, 2021, **15**, 16442.
18 X. Ma, T. Zhang, W. Qiu, M. Liang, Y. Gao, P. Xue, Y. Kang and Z. Xu, *Chem. Eng. J.*, 2021, **420**, 127657.
19 J. Ramos, A. Imaz and J. Forcada, *Polym. Chem.*, 2012, **3**, 852.
20 C. Miao, F. Li, Y. Zuo, R. Wang and Y. Xiong, *RSC Adv.*, 2016, **6**, 3013.
21 D. Huang, H. Qian, H. Qiao, W. Chen, J. Feijen and Z. Zhong, *Expert Opin. Drug Delivery*, 2018, **15**, 703.
22 S. Hajebi, A. Abdollahi, H. Roghani-Mamaqani and M. Salami-Kalajahi, *Langmuir*, 2020, **36**, 2683.
23 E. Cazares-Cortes, A. Espinosa, J. M. Guigner, A. Michel, N. Griffete, C. Wilhelm and C. Ménager, *ACS Appl. Mater. Interfaces*, 2017, **9**, 25775.
24 T. M. Don, K. Y. Lu, L. J. Lin, C. H. Hsu, J. Y. Wu and F. L. Mi, *Mol. Pharm.*, 2017, **14**, 4648.
25 J. M. Knipe, L. E. Strong and N. A. Peppas, *Biomacromolecules*, 2016, **17**, 788.
26 Y. Zou, D. Li, Y. Wang, Z. Ouyang, Y. Peng, H. Tomás, J. Xia, J. Rodrigues, M. Shen and X. Shi, *Bioconjugate Chem.*, 2020, **31**, 907.
27 D. P. Walsh, R. M. Raftery, R. Murphy, G. Chen, A. Heise, F. J. O'Brien and S. A. Cryan, *Biomater. Sci.*, 2021, **9**, 4984.
28 J. O'Dwyer, M. Cullen, S. Fattah, R. Murphy, S. Stefanovic, L. Kovarova, M. Pravda, V. Velebny, A. Heise, G. P. Duffy and S. A. Cryan, *Pharmaceutics*, 2020, **12**, 513.
29 J. Jacobs, D. Pavlovic, H. Prydderch, M. A. Moradi, E. Ibarboure, J. P. A. Heuts, S. Lecommandoux and A. Heise, *J. Am. Chem. Soc.*, 2019, **141**, 12522.
30 D. P. Walsh, R. M. Raftery, I. M. Castano, R. Murphy, B. Cavanagh, A. Heise, F. J. O'Brien and S. A. Cryan, *J. Controlled Release*, 2019, **304**, 191.
31 H. R. Kricheldorf, *Angew. Chem., Int. Ed.*, 2006, **45**, 5752.
32 C. Deng, J. Wu, R. Cheng, F. Meng, H. A. Klok and Z. Zhong, *Prog. Polym. Sci.*, 2014, **39**, 330.

Open Access Article. Published on 10 October 2022. Downloaded on 7/19/2025 11:20:55 AM.
This article is licensed under a Creative Commons Attribution-NonCommercial 3.0 Unported Licence.

33 Z. Jiang, J. Chen, L. Cui, X. Zhuang, J. Ding and X. Chen, *Small Methods*, 2018, **2**, 1700307.
34 J. Ding, F. Shi, C. Xiao, L. Lin, L. Chen and X. Chen, *Polym. Chem.*, 2011, **2**, 2857.
35 F. Shi, J. Ding, C. Xiao, X. Zhuang, C. He, L. Chen and X. Chen, *J. Mater. Chem.*, 2012, **22**, 14168.
36 P. Bilalis, S. Varlas, A. Kiafa, A. Velentzas, D. Stravopodis and H. Iatrou, *J. Polym. Sci., Part A: Polym. Chem.*, 2016, **54**, 1278–1288.
37 T. Xing, B. Lai and L. Yan, *Macromol. Chem. Phys.*, 2013, **214**, 578.
38 J. Chen, J. Ding, Y. Wang, J. Cheng, S. Ji, X. Zhuang and X. Chen, *Adv. Mater.*, 2017, **29**, 1701170.
39 T. Xing, B. Lai, X. Ye and L. Yan, *Macromol. Biosci.*, 2011, **11**, 962.
40 K. Bauri, M. Nandi and P. De, *Polym. Chem.*, 2018, **9**, 1257.
41 W. Xu, J. Ding and X. Chen, *Biomacromolecules*, 2017, **18**, 3291.
42 Y. Zhang, J. Ding, M. Li, X. Chen, C. Xiao, X. Zhuang, Y. Huang and X. Chen, *ACS Appl. Mater. Interfaces*, 2016, **8**, 10673.
43 M. A. Gauthier, *Antioxid. Redox Signal.*, 2014, **21**, 705.
44 M. Chen, D. Liu, F. Liu, Y. Wu, X. Peng and F. Song, *J. Controlled Release*, 2021, **332**, 269.
45 L. Shi, J. Zhang, M. Zhao, S. Tang, X. Cheng, W. Zhang, W. Li, X. Liu, H. Peng and Q. Wang, *Nanoscale*, 2021, **13**, 10748.
46 Y. Y. Wang, S. K. Lai, J. S. Suk, A. Pace, R. Cone and J. Hanes, *Angew. Chem., Int. Ed.*, 2008, **47**, 9726.
47 K. Shiraishi and M. Yokoyama, *Sci. Technol. Adv. Mater.*, 2019, **20**, 324.
48 T. T. H. Thi, E. H. Pilkington, D. H. Nguyen, J. S. Lee, K. D. Park and N. P. Truong, *Polymers*, 2020, **12**, 298.
49 N. Gangloff, J. Ulbricht, T. Lorson, H. Schlaad and R. Luxenhofer, *Chem. Rev.*, 2016, **116**, 1753.
50 H. Yu, N. Ingram, J. V. Rowley, S. Parkinson, D. C. Green, N. J. Warren and P. D. Thornton, *J. Mater. Chem. B*, 2019, **7**, 4217.
51 Y. Chen, Z. Xu, D. Zhu, X. Tao, Y. Gao, H. Zhu, Z. Mao and J. Ling, *J. Colloid Interface Sci.*, 2016, **483**, 201.
52 A. Birke, J. Ling and M. Barz, *Prog. Polym. Sci.*, 2018, **81**, 163.
53 D. Skoulas, V. Stuettgen, R. Gaul, S. A. Cryan, D. J. Brayden and A. Heise, *Biomacromolecules*, 2020, **21**, 2455.
54 Z. S. Clauss and J. R. Kramer, *ACS Appl. Mater. Interfaces*, 2022, **14**, 22781.
55 J. V. Rowley, P. A. Wall, H. Yu, M. J. Howard, D. L. Baker, A. Kulak, D. C. Green and P. D. Thornton, *Polym. Chem.*, 2022, **13**, 100.
56 P. Salas-Ambrosio, A. Tronnet, M. Since, S. Bourgeade-Delmas, J.-L. Stigliani, A. Vax, S. Lecommandoux, B. Dupuy, P. Verhaeghe and C. Bonduelle, *J. Am. Chem. Soc.*, 2021, **143**, 3697.
57 S. K. Lai, Y. Y. Wang and J. Hanes, *Adv. Drug Delivery Rev.*, 2009, **61**, 158.

 This journal is © The Royal Society of Chemistry 2022